First Plasma Wave Observations at Neptune

D. A. GURNETT, W. S. KURTH, R. L. POYNTER, L. J. GRANROTH, I. H. CAIRNS, W. M. MACEK,* S. L. MOSES, F. V. CORONITI, C. F. KENNEL, D. D. BARBOSA

The Voyager 2 plasma wave instrument detected many familiar plasma waves during the encounter with Neptune, including electron plasma oscillations in the solar wind upstream of the bow shock, electrostatic turbulence at the bow shock, and chorus, hiss, electron cyclotron waves, and upper hybrid resonance waves in the inner magnetosphere. Low-frequency radio emissions, believed to be generated by mode conversion from the upper hybrid resonance emissions, were also observed propagating outward in a disklike beam along the magnetic equatorial plane. At the two ring plane crossings many small micrometer-sized dust particles were detected striking the spacecraft. The maximum impact rates were about 280 impacts per second at the inbound ring plane crossing, and about 110 impacts per second at the outbound ring plane crossing. Most of the particles are concentrated in a dense disk, about 1000 kilometers thick, centered on the equatorial plane. However, a broader, more tenuous distribution also extends many tens of thousands of kilometers from the equatorial plane, including over the northern polar region.

THE VOYAGER 2 FLYBY OF NEPTUNE on 25 August 1989 revealed that Neptune has a large and complex magnetosphere. In this report we present the first observations of plasma waves and low-frequency radio emissions in the vicinity of Neptune. The plasma wave (PWS) instrument on Voyager is designed to measure the electric field of plasma waves and radio emissions in the frequency range from 10 Hz to 56.2 kHz. Further information on this instrument is given by Scarf and Gurnett (*1*). To provide a framework for presenting the results, the observations are described approximately in the order in which the phenomena occurred, starting with low-frequency radio emissions detected during the approach to Neptune, and ending with observations during the outbound leg in the vicinity of Neptune's moon, Triton.

Radio emissions. Although the planetary radio astronomy instrument started to detect radio emissions at high frequencies (>100 kHz) as much as 30 days before closest approach (*2*), the plasma wave instrument did not detect radio emissions at low frequencies (<100 kHz) until only a few days before closest approach. Even then the intensities were very weak. The low-frequency radio emissions can be seen in the 5.62- through 56.2-kHz channels of Fig. 1, which shows an overview of the PWS electric field intensities during a 32-hour interval centered on closest approach. The radio emission intensities gradually increase as the spacecraft approaches the planet, reach a broad irregular peak around closest approach, and then gradually decrease as the spacecraft recedes from the planet. The low-frequency limit of the radio emission spectrum is about 5 kHz. At high frequencies the spectrum continues smoothly into the frequency range of the planetary radio astronomy instrument, with no evidence of a high-frequency cutoff. Wideband waveform measurements, which provide very high spectral resolution over the frequency range from 50 Hz to 12 kHz show that the spectrum is usually smooth and continuous, very similar to continuum radiation in Earth's magnetosphere (*3*). In a few cases, narrowband components can be seen with bandwidths of a few percent or less.

In addition to the radial distance dependence evident in Fig. 1, the radio emission intensity is also modulated by the rotation of the planet. This modulation pattern is difficult to analyze near closest approach because of the close proximity to the source and the rapid longitudinal motion of the spacecraft. The best measurements of the rotational modulation are obtained far from the planet, particularly on the outbound leg. The basic pattern is illustrated in Fig. 2, which shows the intensity variations in the 17.8-kHz channel from 27 to 30 August, at a radial distance of 140 to 315 Neptune radii (1 R_N = 24,762 km). The intensity scale in this plot has been expanded to show signals just above threshold. The modulation pattern consists of two bursts every 16 hours. The 16-hour period is consistent with the 16-hour rotation period determined by the planetary radio astronomy instrument (*2*). The two-pulse-per-rotation pattern is believed to arise from a disklike beaming geometry, with the plane of the disk tilted with

D. A. Gurnett, W. S. Kurth, L. J. Granroth, I. H. Cairns, W. M. Macek, Department of Physics and Astronomy, University of Iowa, Iowa City, IA 52242.
R. L. Poynter, Jet Propulsion Laboratory, 4800 Oak Grove Drive, Pasadena, CA 91109.
S. L. Moses, F. V. Coroniti, C. F. Kennel, TRW Space and Technology Group, One Space Park, Redondo Beach, CA 90278.
D. D. Barbosa, Institute of Geophysics and Planetary Physics, University of California, Los Angeles, Los Angeles, CA 90024.

*On leave from Space Research Center, Polish Academy of Sciences, Warsaw, Poland.

respect to the equatorial plane of the planet. In Fig. 2 the radio emission bursts are compared with the magnetic equator crossings obtained from the offset tilted dipole (OTD) model of Neptune's magnetic field (*4*). These comparisons show that the symmetry plane of the radio emission disk lies almost exactly along the magnetic equatorial plane. The latitudinal beamwidth at 17.8 kHz is estimated to be about ±15°. Inspection reveals that a null occurs in each burst, which indicates that the beam may have two lobes, one north and the other south of the magnetic equator.

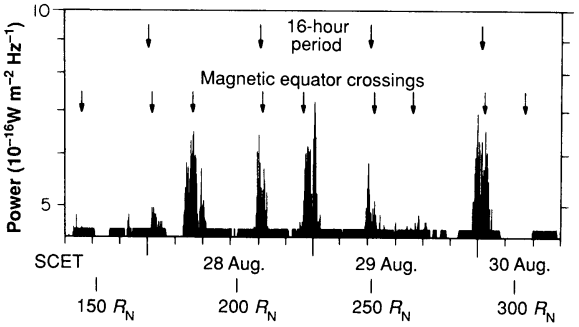

Fig. 2. Periodic bursts of radio noise at 17.8 kHz associated with the rotation of Neptune. The rotational period (upper row of arrows) is about 16 hours, with two bursts of noise per rotation. Times for the magnetic equator crossings (lower row of arrows) are based on the OTD model (*4*).

Upstream waves, bow shock, and magnetopause. The first evidence of plasma waves associated with the bow shock of Neptune's magnetosphere occurred at 1055 spacecraft event time (SCET) on 24 August 1989, while the spacecraft was still in the solar wind upstream of the planet. At this time weak sporadic electron plasma oscillations started to occur in the 562-Hz channel of the plasma wave spectrum analyzer. These oscillations continued for about 1/2 hour and then disappeared. About $1^1/_2$ hours later, at 1252 SCET, the electron plasma oscillations reappeared, this time stronger (~100 μV/m) and more steady. These plasma oscillations can be seen in the 562-Hz channel of Fig. 1. From similar observations at other planets (*5–8*), it is known that electron plasma oscillations are produced by suprathermal electrons escaping into the solar wind from the bow shock. Because the electrons are guided along the solar wind magnetic field, the presence of these waves indicated that the spacecraft was magnetically connected to the bow shock. Furthermore, the relatively high intensities suggested that the spacecraft must be relatively close to the shock. Indeed, about $1^3/_4$ hours later, at 1435 SCET, the plasma wave instrument detected an intense broadband burst of noise that signaled the arrival of the shock. The electric field intensities in this region are shown in greater detail in Fig. 3. The shock can be clearly identified by the abrupt broadband burst of electric field noise in the 10- to 178-Hz channels from about 1435 to 1448 SCET. The shock transition region is relatively thick and has a corresponding signature in the magnetic field (*4*) and plasma (*9*) data at a radial distance from the center of the planet of about 35.0 R_N.

After the shock crossing, the plasma wave electric field intensities dropped to the instrument noise level as the spacecraft entered the magnetosheath, similar to the magnetosheaths at Jupiter, Saturn, and Uranus (*6–8*), which were also very quiet. The magnetometer (*4*) and plasma (*9*) instruments showed that the spacecraft crossed the magnetopause into the magnetosphere during the interval from about 1800 to 1930 SCET. No signature of the magnetopause crossing was evident in the plasma wave data. This situation is in sharp contrast to Jupiter, Saturn, and Uranus, where the magnetopause can be identified by continuum radiation trapped in the low-density cavity formed by the magnetosphere. If trapped continuum radiation exists in Neptune's magnetosphere, then it must be weak, below the detection threshold of the instrument.

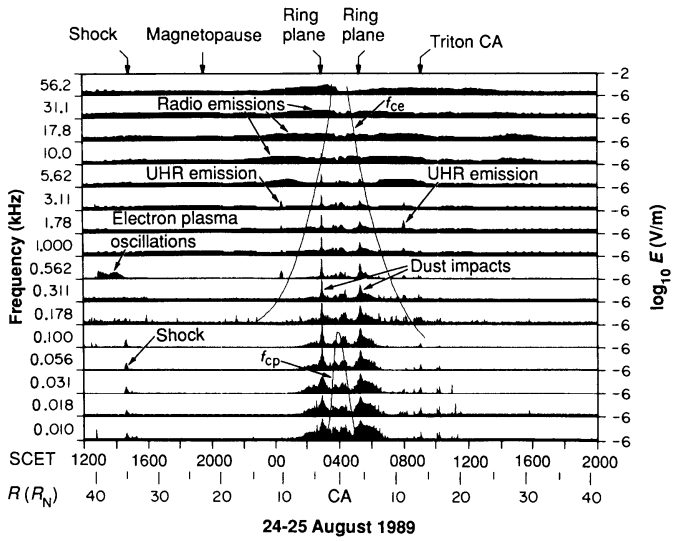

Fig. 1. A 16-channel plot of the electric field intensities from the plasma wave instrument. The horizontal scale is spacecraft event time (SCET). The smooth solid lines labeled f_{ce} and f_{cp} give the electron and proton cyclotron frequency, which were computed from magnetic field data of Ness and colleagues (*4*). The values of the cyclotron frequency inside of about 3 R_N are based on 8-min averages of the magnitude of B, and the values outside of about 3 R_N are based on the OTD model (*4*).

Ring plane. At the ring plane crossing of Saturn it was discovered that the plasma wave instrument and planetary radio astronomy instrument could detect small, micrometer-sized dust particles striking the spacecraft (*10*). When a small particle strikes the spacecraft at a velocity exceeding a few kilometers per second, the particle is instantly vaporized and heated to a high temperature, producing a cloud of ionized gas that expands away from the impact site. As the ionized gas cloud contacts the electric antenna, some of the charge is collected by the antenna, thereby causing a voltage pulse. Laboratory experiments show that the charge released is proportional to the mass of the dust particle. The amplitude of the voltage pulse is therefore proportional to the mass of the impacting particle.

Since Neptune was known to have a ring system, it was anticipated that the plasma wave instrument would detect dust impacts at the ring plane crossings. Indeed this was the case. Two ring plane crossings occurred during the Neptune flyby, one on the inbound leg shortly before closest approach, and the other on the outbound leg shortly after closest approach. The locations of the two ring plane crossings are indicated at the top of Fig. 1. At each ring plane an intense broadband burst of noise can be seen in nearly all channels, extending from below 10 Hz to above 10 kHz. This noise is caused by dust impacts on the spacecraft. The peak intensity detected at the inbound and outbound ring plane crossings occurred at 0253:19 ± 4 s and 0516:07 ± 4 s SCET, respectively. Two components can be seen. The most intense component is sharply peaked at the ring plane and has a duration of about 10 min. The second weaker component extends over a broad region, beginning about 1 hour before the first ring plane crossing and ending about 1 hour after the second ring plane crossing. Impact noise was even detected over the polar region, between the two ring plane crossings. These data suggest that a dense, thin disk of dust about 1000 km thick exists along the equatorial plane, surrounded by a tenuous halo extending many tens of thousands of kilom-

eters on either side of the equatorial plane.

To provide higher resolution of the dust impacts, a series of wideband plasma wave frames was collected at each of the ring plane crossings. These frames give 48-s samples of the antenna voltage waveform at a sample rate of 28,800 samples per second. A typical impact waveform is shown in Fig. 4. The general characteristics of the waveforms are similar to those observed at Saturn and Uranus. Based on these similarities we assume that the particles detected at Neptune are of similar size (that is, diameters of a few micrometers or less). Further study will be required to more accurately determine the mass and size distribution. Because individual impacts can be detected, accurate measurements can be made of the impact rate as the spacecraft passed through the ring plane. During the inbound ring plane crossing the maximum impact rate was about 280 impacts per second, and during the outbound ring plane crossing the maximum impact rate was about 110 impacts per second. By using the nominal values for the spacecraft velocity and cross-sectional area of the spacecraft, we find that these impact rates imply maximum number densities on the order of 10^{-3} particles per cubic meter.

Inner magnetosphere. The plasma wave intensities in the inner magnetosphere are summarized in Fig. 5, which shows a spectrogram for a 10-hour period centered on closest approach. The intensities in this region are generally quite low, and tend to be dominated by radio emissions at high frequencies and dust impact noise at low frequencies. A brief well-defined narrowband emission can be seen in the 3.11-kHz channel at about 0025 SCET on the inbound leg, and again in the 1.78-kHz channel at about 0800 SCET on the outbound leg. From similar observations at Jupiter, Saturn, and Uranus (*6–8*), these emissions are identified as electrostatic upper hybrid resonance (UHR) waves. UHR waves occur at the upper hybrid resonance frequency, which is given by $f_{UHR} = (f_{ce}^2 + f_{pe}^2)^{1/2}$, where f_{ce} is the electron cyclotron frequency ($f_{ce} = 28B$ Hz, where B is the magnetic field strength in nanotesla), and f_{pe} is the electron plasma frequency ($f_{pe} = 9000\sqrt{N}$ Hz, where N is the electron density in electrons per cubic centimeter). Comparisons with the magnetometer data (*4*) show that the UHR waves are located very close to the magnetic equator, which is consistent with similar observations at Jupiter, Saturn, and Uranus (*6–8*). Because the electron cyclotron frequency can be computed from the magnetic field measurements (*3*), the UHR emission frequency provides a direct measurement of the electron density. The electron densities are 0.12 cm^{-3} at 0025 SCET and 0.04 cm^{-3} at 0800 SCET. Enhanced electric field intensities can also be seen in Fig. 5 slightly above the electron cyclotron frequency at 0025 and 0800 SCET, in the same region where the UHR emissions occur. These emissions are believed to be electrostatic electron cyclotron waves. Electron cyclotron waves occur near half-integral harmonics of the electron frequency (that is, $3f_{ce}/2$, $5f_{ce}/2$, and so on) and are generated by the same type of equatorially trapped electron distributions that produce the UHR emissions.

The low-frequency radio emissions reach maximum intensity at about the same time that the UHR emissions occur (that is, near the magnetic equator) (Fig. 5). For many years it has been known that planetary radio emissions can be produced in the free space left-hand ordinary (L-O) wave mode by mode conversion from electrostatic UHR waves (*11*). These observations therefore lead us to believe that the low-frequency continuum-like radio emissions are generated by mode conversion from the equatorial UHR emissions. This conclusion is further supported by the fact that the radio emissions continue smoothly across the electron cyclotron frequency, which shows that they are propagating in the L-O mode.

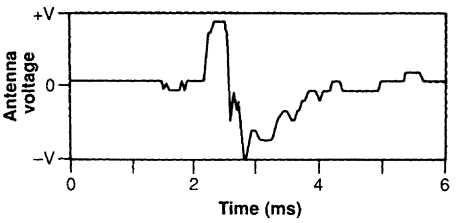

Fig. 4. An antenna voltage waveform of a dust impact detected by the plasma wave wideband receiver near the first ring plane crossing.

Near closest approach, around 0400 SCET and shortly thereafter, numerous complex radio and plasma wave emissions can be seen extending across the entire spectrum. The analysis of these waves is complicated by the nondipolar nature of the magnetic field (*4*) and by large uncertainties in the electron densities. The spacecraft coordinates are also changing rapidly in this region. For example, the magnetic latitude (λ_m) from the OTD magnetic field model varies from near the magnetic pole ($\lambda_m = 76.4°$) to the magnetic equator ($\lambda_m = 0°$) in less than 1 hour, from 0339 to 0421 SCET. A series of high-resolution wideband frames was obtained shortly after closest approach, which greatly aided the interpretation of the data. Some of these frames are illustrated in Fig. 6, which shows a mosaic of twelve 48-s wideband spectrograms extending from 0405:36 to 0433:36 SCET. The most prominent feature in these spectrograms is a narrowband emission slightly above 3 kHz that extends across the entire time interval. The frequency of the emission increases slightly, from about 3.3 kHz at the beginning to about 3.8 kHz at the end. Since this frequency is well below the electron cyclotron frequency, which varies from about 215 to 55 kHz during this period (*4*), the emission could be a whistler-mode emission. However, the near constancy of the emission frequency over such a large range of magnetic latitudes makes us believe that this interpretation is unlikely. More likely, the signal is caused by a radio emission that has propagated to the spacecraft from a remote source at a frequency above the local electron plasma frequency (that is, the free space L-O mode). Somewhat similar narrowband radio emissions have been observed at Saturn (*7*). A more likely candidate for a whistler-mode emission can be seen below 1 kHz in the frames beginning at 0411:23, 0412:47, and 0415:11 SCET. These emissions have spectral features similar to whistler-mode hiss and chorus in other planetary magnetospheres (*6–8*). If these emissions are whistler-mode waves, they are most likely generated by cyclotron resonance interactions

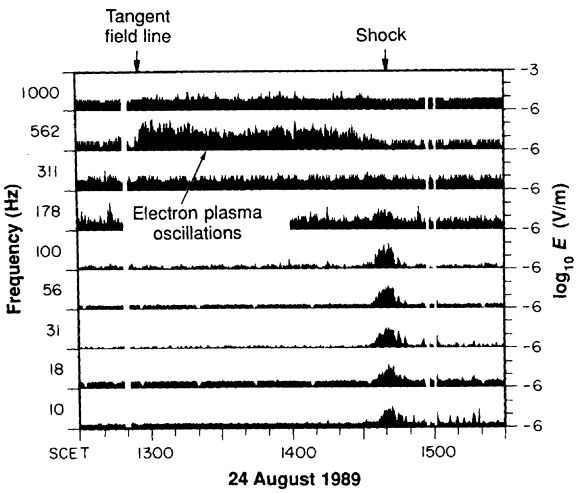

Fig. 3. An expanded-scale plot showing the upstream electron plasma oscillations and the intense broadband burst of electric field noise at the bow shock.

with energetic electrons trapped in Neptune's radiation belt (*12*).

Strong emissions are present in the frequency range from about 10 to 31 Hz around closest approach (Fig. 5). These emissions are below the proton cyclotron frequency and are in a frequency range where they could be attributed to electrostatic or electromagnetic ion cyclotron waves. If these emissions are ion cyclotron waves, they may play an important role in the scattering and loss of energetic ions from the radiation belt.

A search was also conducted for signals called "whistlers" that are generated by lightning. Whistlers produced by terrestrial lightning have been studied for many years in Earth's magnetosphere (*13*). Similar signals from Jovian lightning were also observed by Voyager 1 in the magnetosphere of Jupiter (*6*). Although several events were detected in the magnetosphere of Neptune with characteristics similar to whistlers, the dispersion of these signals proved to be so large (20,000 $s^{1/2}$) that they are not believed to have originated from lightning. Such large dispersions would require path lengths and plasma densities that are much larger than anything plausible in the Neptunian magnetosphere. Further study is required to determine the origin of these signals.

Triton. During the outbound leg, numerous brief bursts of broadband electric field noise were observed at frequencies from 10 to 100 Hz during the period of approach to Triton from about 0820 to 0910 SCET on 25 August at radial distances ranging from 12.4 to 14.5 R_N (Fig. 1). No comparable noise bursts were observed in the same radial distance range on the inbound leg. Some of these bursts are caused by interference from the spacecraft attitude control thrusters. However, it is not clear that all of the noise bursts in this region can be attributed to thruster firings and other known interference effects. Since these emissions occur in the vicinity of Triton, they could possibly be caused by an interaction of Triton's atmosphere with the magnetosphere of Neptune, similar to the interaction of Saturn's moon, Titan, with the magnetosphere of Saturn (*7*).

On strictly geometric grounds, the flyby of Triton is not favorable for detecting an interaction of Triton with the magnetosphere of Neptune. The radial distance at closest approach to Triton (0910 SCET) is 29.4 Triton radii, which is quite large. Furthermore, for a corotating magnetosphere, the flow velocity is such that the spacecraft passed upstream of Triton, which is not suitable for detecting wake effects. Despite these unfavorable conditions, there have been cases where satellite interaction effects have been observed in highly unusual geometries because of the long distance propagation of Alfvén waves and other effects (*14*). Further study and comparisons with data from other instruments will be needed to determine if any of these noise bursts could be associated with Triton.

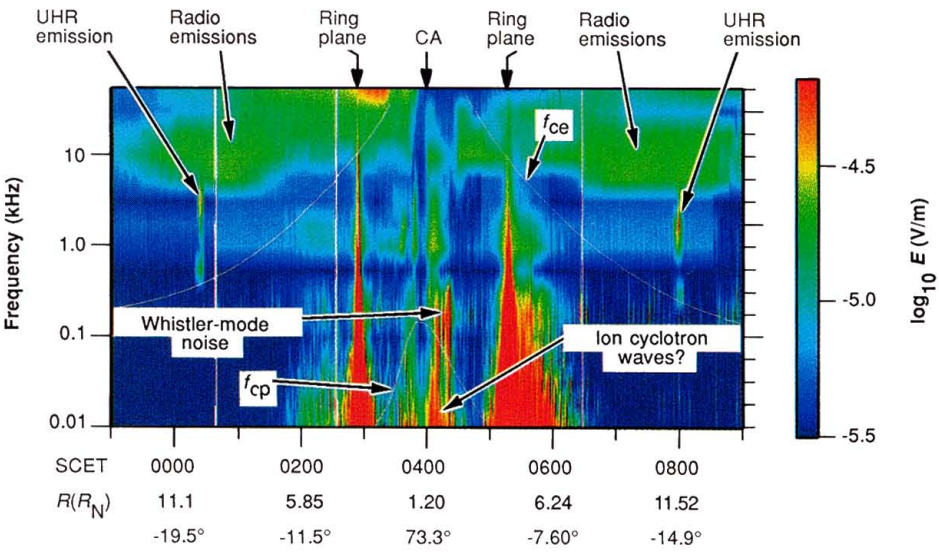

Fig. 5. A frequency-time spectrogram summarizing the electric field intensities observed in the inner magnetosphere with the use of measurements from the 16-channel spectrum analyzer. The intensities have been averaged and smoothed to produce a continuous spectrum. The profiles of f_{ce} and f_{cp} are derived from the magnetic field data (*4*), as in Fig. 1.

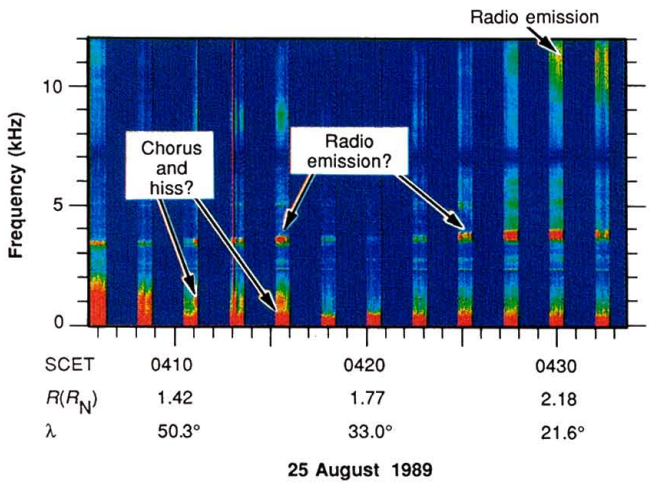

Fig. 6. A mosaic of twelve 48-s frequency-time spectrograms obtained from the wideband receiver shortly after closest approach to Neptune.

REFERENCES AND NOTES

1. F. L. Scarf and D. A. Gurnett, *Space Sci. Rev.* **21**, 289 (1977).
2. J. W. Warwick *et al.*, *Science* **246**, 1498 (1989).
3. D. A. Gurnett, *J. Geophys. Res.* **80**, 2751 (1975).
4. N. F. Ness *et al.*, *Science* **246**, 1473 (1989).
5. F. L. Scarf, R. W. Fredricks, L. A. Frank, M. Neugebauer, *J. Geophys. Res.* **76**, 5162 (1971).
6. F. L. Scarf, D. A. Gurnett, W. S. Kurth, *Science* **204**, 991 (1979).
7. D. A. Gurnett, W. S. Kurth, F. L. Scarf, *ibid.* **212**, 235 (1981).
8. ———, R. L. Poynter, *ibid.* **233**, 106 (1986).
9. J. W. Belcher *et al.*, *ibid.* **246**, 1478 (1989).
10. F. L. Scarf, D. A. Gurnett, W. S. Kurth, R. L. Poynter, *ibid.* **215**, 587 (1982); J. W. Warwick *et al.*, *ibid.*, p. 582.
11. D. A. Gurnett and L. A. Frank, *J. Geophys. Res.* **81**, 3875 (1976); D. Jones, *Nature* **260**, 686 (1976); K. H. Rönnmark *et al.*, *Space Sci. Rev.* **22**, 401 (1978); D. Jones, *Nature* **288**, 225 (1980); W. S. Kurth, D. A. Gurnett, R. R. Anderson, *J. Geophys. Res.* **86**, 5519 (1981); D. Barbosa, *Rev. Geophys.* **20**, 316 (1980).
12. S. M. Krimigis *et al.*, *Science* **246**, 1483 (1989).
13. R. A. Helliwell, *Whitlers and Related Ionospheric Phenomena* (Stanford Univ. Press, Stanford, CA, 1965).
14. A. Eviatar, G. L. Siscoe, J. D. Scudder, E. C. Sittler, Jr., J. D. Sullivan, *J. Geophys. Res.* **87**, 8091 (1982); E. J. Smith and B. T. Tsurutani, *ibid.* **88**, 7831 (1983).

15. We thank the Voyager team at the Jet Propulsion Laboratory (JPL) and the staff at National Aeronautics and Space Administration (NASA) headquarters for valuable support. We are especially grateful to E. Miner for scheduling the wideband coverage and to P. Liggett and the staff of the JPL VNESSA facility for providing near real-time processing. We thank N. Toy and the JPL General Science Data Team for timely and efficient production of experiment data records. We also thank J. P. de Vries and the Flight Science Office for continuous support throughout the Neptune phase of the mission; J. Cook-Granroth for compiling the various data products into com-

prehensible form; and J. Belcher, S. Krimigis, N. Ness, and J. Warwick for helpful discussions concerning the interpretation of the data. Finally, we remember and acknowledge the vital contribution of the late F. L. Scarf, who was principal investigator of the plasma wave team until his death in July 1988. Research at the University of Iowa was supported by NASA through contract 957723 with JPL, and by the state of Iowa through a faculty developmental assignment for one of the authors (D.A.G.). Research at TRW was supported by NASA through contract 957805 with JPL.

30 October 1989; accepted 15 November 1989